Journal of Power Sources 257 (2014) 163–169

Contents lists available at ScienceDirect

Journal of Power Sources

journal homepage: www.elsevier.com/locate/jpowsour

The effect of fluoroethylene carbonate additive content on the formation of the solid-electrolyte interphase and capacity fade of Li-ion full-cell employing nano Si–graphene composite anodes

Arnaud Bordes, KwangSup Eom*, Thomas F. Fuller

School of Chemical & Bimolecular Engineering, Center for Innovative Fuel Cell and Battery Technologies, Georgia Institute of Technology, Atlanta, GA 30332, USA

HIGHLIGHTS

- Li ion full cells employing Si–graphene anodes were used in this study.
- FEC additive improves cyclability of the full-cell by formation of good SEI.
- 5 wt.% FEC is optimum with high capacity and low capacity fade.
- 5 wt.% FEC forms less amount of SEI compounds consuming Li^+.

ARTICLE INFO

Article history:
Received 8 November 2013
Received in revised form
6 December 2013
Accepted 11 December 2013
Available online 2 February 2014

Keywords:
Li ion battery
Full cell
Silicon–graphene composite
Solid-electrolyte interphase
Fluoro-ethylene carbonate
Lithium nickel cobalt aluminum oxide cathode

ABSTRACT

When fluoroethylene carbonate (FEC) is added to the ethylene carbonate (EC)–diethyl carbonate (DEC) electrolyte, the capacity and cyclability of full-cells employing Si–graphene anode and lithium nickel cobalt aluminum oxide cathode (NCA) cathode are improved due to formation of a thin (30–50 nm) SEI layer with low ionic resistance ($\sim$2 ohm cm^2) on the surface of Si–graphene anode. These properties are confirmed with electrochemical impedance spectroscopy and a cross-sectional image analysis using Focused Ion Beam (FIB)-SEM. Approximately 5 wt.% FEC in EC:DEC (1:1 wt.%) shows the highest capacity and most stability. This high capacity and low capacity fade is attributed to a more stable SEI layer containing less CH_2OCO_2Li, Li_2CO_3 and LiF compounds, which consume cyclable Li. Additionally, a greater amount of polycarbonate (PC), which is known to form a more robust passivation layer, thus reducing further reduction of electrolyte, is confirmed with X-ray photoelectron spectroscopy (XPS).

1. Introduction

Lithium-ion batteries (LIBs) are the power source of choice for both portable devices and electric vehicles [1,2]. In order for electrical vehicles with LIBs to be embraced more fully, the specific energy of LIBs needs to be improved without sacrificing safety, material availability, and cost. Silicon, as a negative electrode material with various morphologies or nanostructures, is one possible solution because lithiated silicon provides high specific energy (4200 mAh g^{-1}) and is an earth abundant material [3–5]. However, silicon expands up to 300% during lithiation. Repeated non-uniform dilation and contraction pulverizes the silicon, leading to a loss of electrical contact and rapid capacity fading [6]. One mitigation is to form a silicon–graphene composite. The graphene is used as a buffer material and enhances electrical conductivity of the electrode [7–16]. Even so, loss of electrical conductivity is not the only cause of capacity fading. Indeed, several mechanisms, such as phase change, insertion of solvated lithium, and electrolyte reduction throughout cycling, can also contribute to irreversible loss of capacity [17,18]. The last two phenomena, although not avoided completely, are at least controlled by the formation of a stable solid electrolyte interphase (SEI) on the surface of electrode during formation [19–22].

Thus, the quality of SEI is a major factor that determines capacity and power capability, lithium deposit morphology, and cyclability. A good SEI should be uniform, adhere well to the anode, and have

* Corresponding author. Tel.: +1 404 747 0451.
E-mail addresses: keom@gatech.edu, kwangsup.eom@gmail.com (K. Eom).

0378-7753/$ – see front matter © 2014 Elsevier B.V. All rights reserved.
http://dx.doi.org/10.1016/j.jpowsour.2013.12.144

high ionic and electrical conductivity [19–22]. The SEI is formed from the reduction and polymerization of the electrolyte solvents. Additives to the electrolyte can improve the quality and composition of the SEI [23–27]. Specifically, fluoro-ethylene carbonate (FEC) has been shown to be effective in reducing irreversible capacity loss and lowering capacity fade for several carbon and silicon based anode materials [23–27]. The effect of FEC additives on Si–graphene anodes has been reported only for half-cells. In contrast to half cells with a lithium foil counter electrode, with full-cells using practical electrodes there is a limited supply of lithium provided by the positive electrode. Therefore, in addition to the increase in internal resistance of the cell attributed to SEI formation [26], lithium consumed in the formation of the SEI is no longer available for cycling. The effect of the FEC additive on the properties of the SEI layer formed on the Si–graphene anode is not yet fully understood, and the optimization of the FEC contents has not yet been investigated, especially in the full-cells.

For these reasons, the optimal content of FEC additive was investigated in order to enhance the performance of a Li-ion full-cell battery using nano Si–graphene composite anode and NCA ($Li[Ni_{0.8}Co_{0.15}Al_{0.05}]O_2$) cathode. The influence of the FEC on the electrochemical and morphological behavior of the SEI layer formed on Si–graphene anode was specifically studied using the electrochemical impedance spectroscopy (EIS), Focused Ion Beam (FIB)-Scanning Electron Microscopy (SEM), and X-ray Photoelectron Spectroscopy (XPS).

2. Experimental methods

2.1. Electrode preparation

In this study, we used a Si–graphene negative electrode and a $Li[Ni_{0.8}Co_{0.15}Al_{0.05}]O_2$ (NCA) positive electrode for the full-cells. The Si–graphene electrode is composed of nano-spherical Si particles, nano-sized multi-layered plate-like graphene, and polyacrylic acid (PAA) binder (*Sigma Aldrich*) and conductive additive of micro-sized multi-layered graphene [26]. NCA with a graphitic carbon conductive additive and polyvinylidenefluoride (PVdF) binder formed the positive electrode [26].

2.2. Cell assembly

All full-cells were fabricated as pouch-type cells with an active area of 9 cm^2. The mass loadings of active material (anode:cathode) were 0.0141 g:0.131 g, indicating that the design capacity of anode is 1.15 times more than that of cathode based on the measured capacity in half cells after the 1st formation cycle [26]. The electrolyte used was EC:DEC = 1:1 (wt.%) with 1 M $LiPF_6$, and the electrolyte of 2.5 ml was applied for one pouch cell. To investigate the effect of FEC content on the cycling behavior of the cells, 0 to 20 wt.% of FEC was added to the EC–DEC electrolyte. A microporous trilayer membrane (*Celgard 2325*) was used as a separator. The half cell used in this study was composed of the Si–graphene electrode and extra pure Li metal (reference/counter) with active area of 1.584 cm^2.

2.3. Electrochemical analysis

To characterize the electrochemical properties of the full-cells, capacity–voltage (C–V) tests were performed at C/15 for the 1st charge and discharge cycle and C/2 for subsequent cycles. The C/15 is based on theoretical capacity and C/2 on measured 1st cycle capacity. All cycling tests were conducted at room temperature (~20 °C) using an *Arbin* battery cycler. The full-cells were charged to 4.2 V at constant current (CC) and then held at constant voltage (CV) until the current was half of applied C-rate. Discharges were done at CC to a cut-off potential of 2.75 V.

Electrochemical Impedance Spectroscopy (EIS) of full-cells was conducted at either a nearly full state of charge (SOC) of 4.09–4.12 V or in the fully discharged state of 3.0–3.1 V using a potentiostat. The frequency was scanned from 1 MHz–0.01 Hz using a 5 mV amplitude perturbation. The values for resistances of individual components were determined with a fitting program. The half cells of Si–graphene electrode were cycled between 0.05 and 1.0 $V_{Li+/Li}$. The EIS tests of the half cells were performed at fully charged (delithiated electrode) states of 0.75–0.78 $V_{Li+/Li}$.

2.4. Postmortem analysis

For surface characterization, the cells were opened in an Ar-filled glove box and washed gently for 5 min in extra pure dimethyl carbonate (DMC) solvent (*Sigma Aldrich*) to remove Li salts, and the samples were stored in the packs filled with Ar before analysis.

To observe the morphologies of the surface of the electrodes, the High Resolution (HR)-SEM (*Hitachi SU8000*) was used. To observe the morphologies of SEI layers and measure the thickness, the electrode surfaces were cut with cubic shapes ($10 \times 10 \times 5$ μm) by a focused ion beam (FIB), and then the inside cross-section was observed using a SEM (*Nova nanolab FEI 200*).

To examine the compounds of SEI compound, X-ray photoelectron spectroscopy (*Kratos XPS*) analysis was performed. The obtained XPS peaks were separated into several peaks with a fitting program (*XPS Peak*), and then the separated peaks were confirmed as individual chemical components by indexing the binding energy.

3. Results and discussion

3.1. Effect of FEC content on the formation cycle and capacity fade

Fig. 1(a) shows the capacity fade of the full-cells (anode: Si–graphene, cathode: NCA) for 0, 5, 10, and 20 wt.% FEC in EC:DEC (1:1 wt.%) electrolyte with 1 M $LiPF_6$. The cell was charged and discharged at C/2 except for 1st cycle (C/15). The cell with 5% FEC showed the highest capacity and highest capacity retention through 50 cycles. The values of charge capacity and capacity retention are summarized in Table 1. Whereas the charge capacity of the cell with 5% FEC increased slightly as shown in Fig. 1(b), the charge capacity of the other cells decreased by an average of 25.6% between the 1st and 2nd charges. Although the cell with 5% FEC showed a large decrease in 1st discharge capacity similar to the others, its capacity was almost recovered beginning with the 2nd charge cycle. This behavior is considered likely due to complete formation of more stable SEI layer in the 1st discharge cycle of the cell with 5% FEC. It is evident that the cell with 5% FEC exhibited higher coulombic efficiency than the cell without FEC, especially during the first ten cycles (Fig. 1(c and d)). In particular, the efficiency of the cell with 5% FEC exceeded 99.0% after the 3rd cycle.

The cells with 10% and 20% FEC behaved the same as the cell without FEC on the 1st cycle, but after the 3rd cycle the capacities for cells with FEC recovered slightly and then stabilized. These data indicate that the SEI layer becomes stable after 5 cycles. After 25 cycles, the capacity of the cells with 10 and 20% FEC was about 15% lower than that for the 5% FEC cell, but more than 16% higher than that the cell without FEC (0% FEC). After the initial cycles, the rate of capacity decrease was similar for all cells.

From the above results, it is notable that FEC additive can improve the initial irreversible capacity loss of the full-cell employing Si–graphene anode during initial formation cycling.

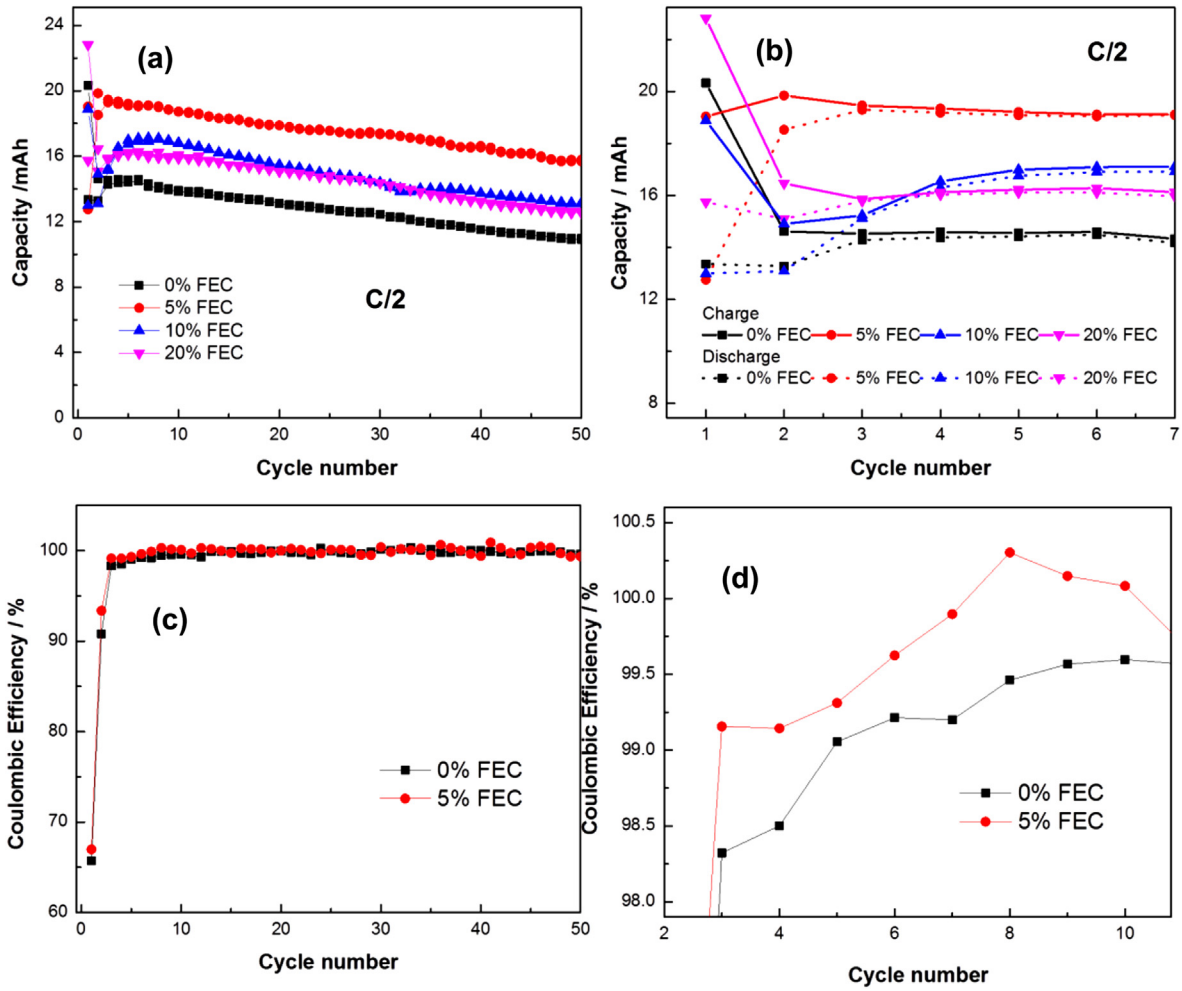

Fig. 1. (a) Capacity fade of the full pouch cells containing 0, 5, 10 or 20% FEC in the EC–DEC (1:1 wt.%) electrolyte over 50 cycles. (b) Close-up of (a) during first 7 cycles showing both charge and discharge capacity. (c) Coulombic efficiency for the full pouch cell containing 0 and 5% FEC in the EC–DEC electrolyte, and (d) close-up during first 10 cycles.

Furthermore, 5% FEC is more effective than higher contents of FEC (10% and 20%).

According to the reaction pathway proposed by Etacheri et al., [23], polycarbonate (PC) is formed through the polymerization of vinylene carbonates (Re. 2), which is generated by the decomposition of FEC (Re. 1)

$$\text{FEC} + \text{R–O Li}^{+} \rightarrow \text{VC (vinylene carbonate)} + \text{R–OH} + \text{LiF} \quad \text{(Re.1)}$$

$$[\text{VC}]_{n} + \text{ne}^{-} \rightarrow \text{PC (polycarbonate)} \quad \text{(Re.2)}$$

Polycarbonate (PC) is an electrochemically and structurally stable polymer, and hence a good SEI compound with high stability [23]. However, concomitant with the formation of PC, LiF is produced from the elimination of HF from FEC (Re. 1). Because the amount of Li ions of the full-cell is limited by the positive electrode, the consumption of Li ions can affect directly the cell capacity.

Table 1
Charged capacity and capacity fade ratio of the full-cells (anode: Si–graphene, Cathode: NCA) with various FEC additive contents in the EC–DEC (1:1 wt.%) electrolyte during 50 cycles.

FEC content in the EC–DEC electrolyte	Charged/Discharge capacity/mAh				Capacity fade ratio from 1st to 50th cycle/%
	1st	2nd	25th	50th	
0%	20.3/13.4	14.6/13.3	12.7/12.7	11.0/10.9	45.8%
5%	19.0/12.8	19.8/18.5	17.6/17.6	15.8/15.7	18.2%
10%	18.9/13.0	14.9/13.1	14.9/14.9	13.2/13.1	30.2%
20%	22.8/15.7	16.5/15.1	14.8/14.7	12.6/12.5	44.7%

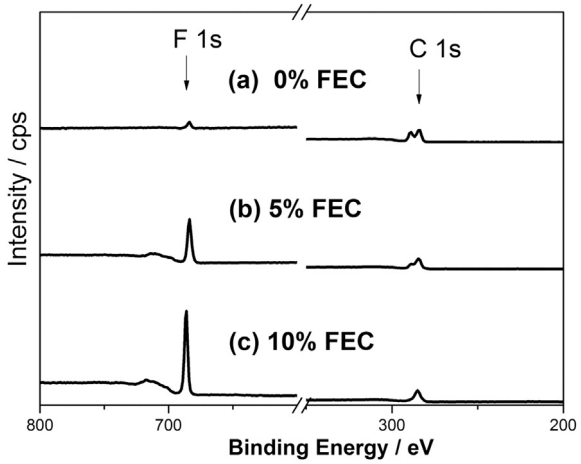

Fig. 2. XPS survey (C 1s and F 1s) of 50th cycled Si–graphene anode from the full-cells employing NCA cathode with (a) 0%, (b) 5%, (c) 10% FEC additive content in the EC–DEC electrolyte.

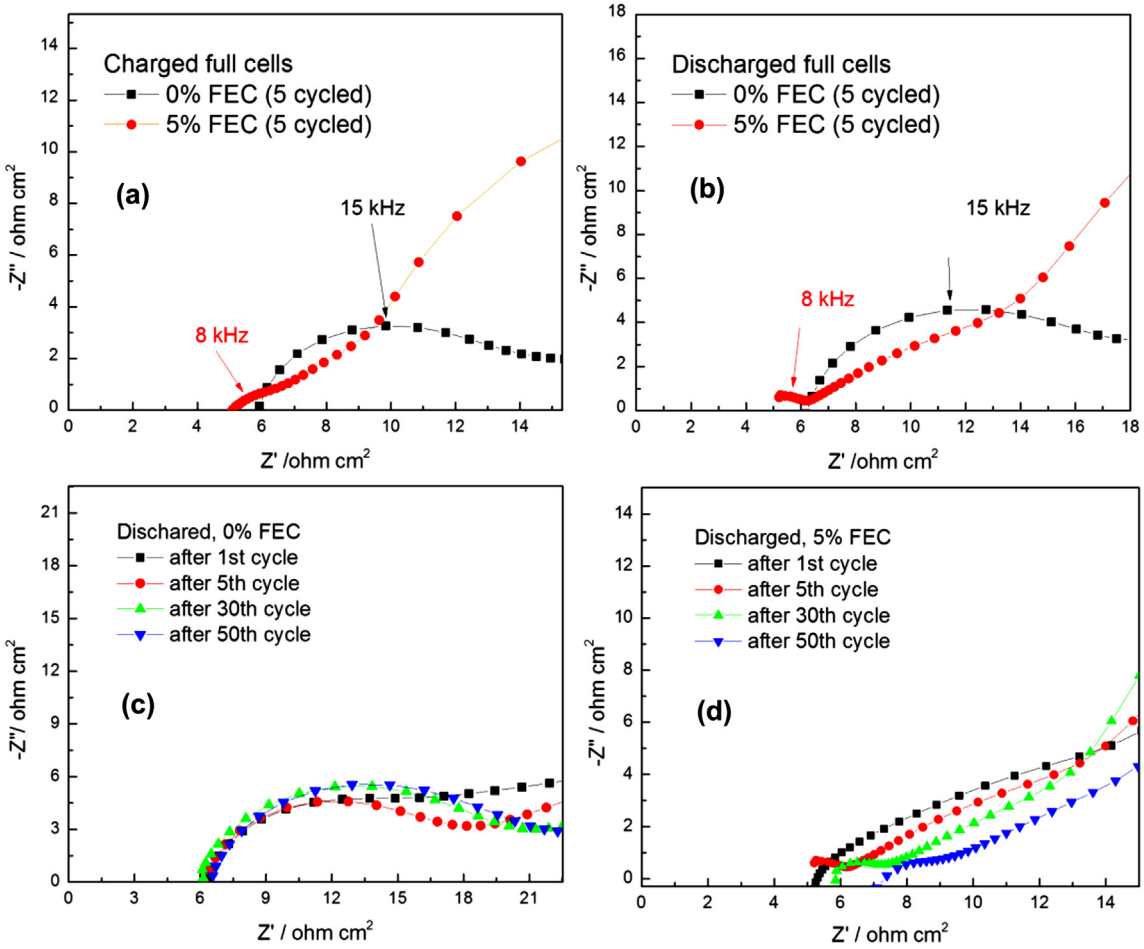

Fig. 3. EIS Nyquist plots of the 5th cycled (a) charged and (b) discharged full-cells with 0% and 5% FEC in the EC–DEC electrolyte. Effects of cycling on the EIS Nyquist plot of discharged full-cells (c) with 0% FEC and (d) 5% FEC in the electrolyte.

As shown in the XPS survey of the cell after 50 cycles (Fig. 2), it was found that with increasing FEC content from 0 to 10%, the intensity of F 1s peak at 685 eV, corresponding to LiF (684.8–685.1 eV), increased relative to that of C 1s peak. This comparative growth indicates that more cyclable Li is consumed with increasing in FEC content. Consequently, the cells with more than 10 wt.% FEC in the EC–DEC electrolyte were expected to have a lower initial capacity compared to cells with 5% FEC due to the greater consumption of the Li in the full-cell. However, a cell with 2.5 wt.% FEC showed no improvement compared to a cell without FEC (the data are not presented in this manuscript). It is suspected that with too low of an FEC content, a dense, complete SEI layer is not formed. Therefore, it was concluded that 5% FEC is near optimal to improve the cyclability of the full-cells employing the Si–graphene anode.

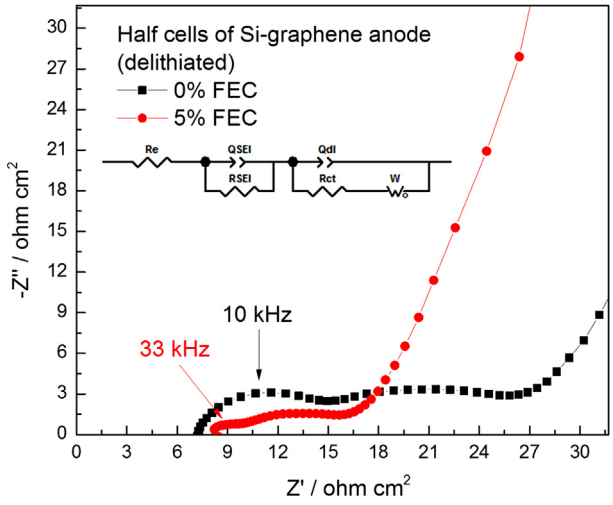

Fig. 4. EIS Nyquist plots of the 5th cycled and delithiated half Si–graphene cell with 0% and 5% FEC in the EC–DEC electrolyte (inside: equivalent circuit for EIS fitting).

3.2. *Effect of FEC additive on the SEI resistances of full-cells (by EIS)*

EIS is a powerful tool to investigate the kinetics of reactions and diffusion processes occurring in the electrodes, surface films, and electrolyte [28–30]. A typical Nyquist plot for the full-cell Li-ion battery consists of a high-frequency Z_{im}-intercept, first high-

Table 2
The resistances of Solid-Electrolyte-Interface (SEI) layers of the full-cells (anode: Si–graphene composite, cathode: NCA) with 0% and 5% FEC after various cycles, which is from the fitting results of Nyquist plots of Fig. 3(c) and (d).

Number of cycle	R_{SEI}/ohm cm^2	
	0% FEC	5% FEC
1	12.4	0.83
5	11.7	1.86
30	15.3	1.89
50	15.4	2.25

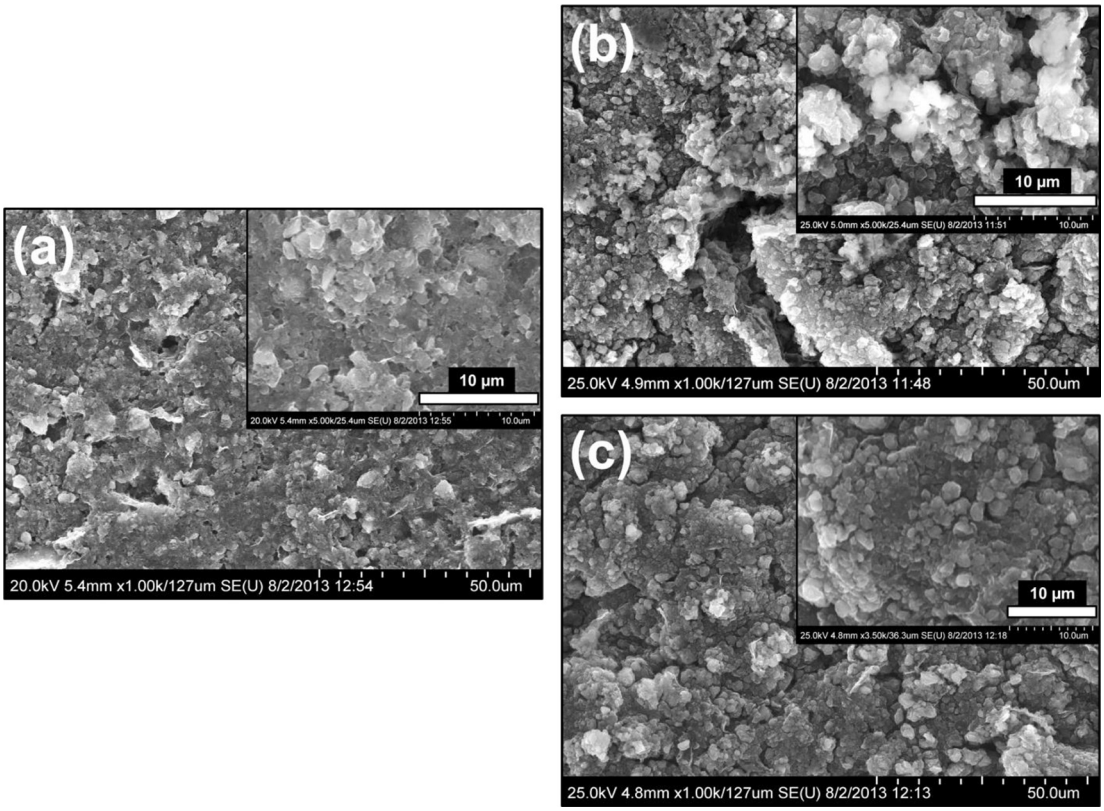

Fig. 5. HR-SEM surface morphologies of Si–graphene anode (a) before and after 50th cycling from the discharged pouch full-cells with (b) 0% FEC and (c) 5% FEC in the EC–DEC (1:1 wt.%) electrolyte.

frequency semi-circle, the second middle-frequency semi-circle, and a low-frequency curve. These features are roughly attributed to the resistances of electrolyte, the SEI films (mostly on negative electrode), the charge-transfer resistance, and diffusion, respectively [26,28]. In order to estimate the SEI resistance, the focus was on the evolution of the 1st semi-circle in the high-frequency range between 1 MHz and 1 kHz. Fig. 3 (a) and (b) shows the Nyquist plots after the 5th cycle of charged and discharged full-cells, respectively. The SEI resistances (R_{SEI}) of charged full-cells with 0% FEC and 5% FEC were 7.84 and 2.10 ohm-cm^2, and those of discharged full-cells were 11.7 and 1.86 ohm-cm^2. From the Nyquist plot of delithiated (5th cycled) half Si–graphene cells of Fig. 4, the R_{SEI} was 8.1 ohm-cm^2 and 2.2 ohm-cm^2 in the cell with 0% and 5% FEC, respectively, which is similar to the values of full-cells, leading to the fact that the R_{SEI} of the full-cell is mostly affected by the Si–graphene anode. Moreover, it is notable that the R_{SEI} of the cell with 5% FEC is 4–6 times smaller than that for the cell without FEC (0% FEC), indicating that FEC additive can result in an SEI layer with improved the ionic resistance.

From the Nyquist plots of Fig. 3(c) and (d), it was found that with an increase in number of cycle (1–50), the R_{SEI} increased slightly. The values were summarized in Table 2. After 50 cycles, the R_{SEI} of the cell without FEC increased to 15.4 ohm-cm^2 and the resistance for 5% FEC increased to 2.25 ohm-cm^2. Nonetheless, the value of SEI resistance for the cell with 5% FEC was still small, and 6.8 times lower than that for the cell without FEC. These results indicate that the positive impact of the addition of FEC, which improve the ionic conductivity of SEI layer, is effective for at least 50 cycles. This behavior can support the fact that the capacity after 50 cycles of the cell with 5% FEC (1.70 mAh) is higher than that without FEC (1.18 mAh) as shown in Fig. 1(a) and Table 1.

3.3. *Effect of FEC additive on the morphology of Si–graphene anode*

SEM images, Fig. 5(a)–(c), show the surface morphology of the Si–graphene composite anode in the pristine state and after 50 cycles for full-cells with 0% FEC and 5% FEC. As shown in Fig. 5(b), on the anode without FEC (0% FEC), an abundant, bright, oxide layer covered the surface of the anode randomly; and a crack of 10 μm in width was seen on the surface. However, after 50 cycles the surface of the Si–graphene anode with 5% FEC was almost unchanged compared to pristine material (Fig. 5(a)). It was thought that abundant SEI-like oxide layer made the Si–graphene surface

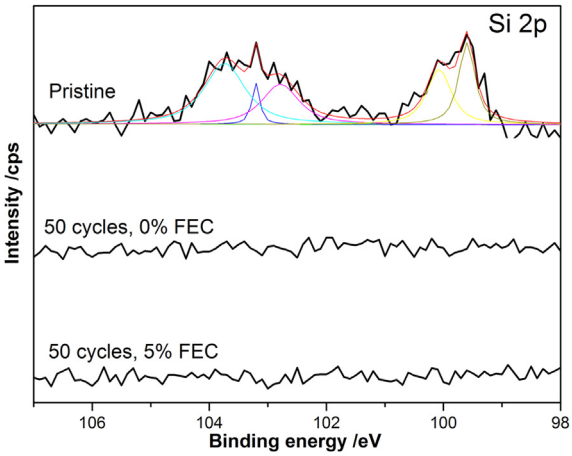

Fig. 6. X-ray photo-electron spectroscopy (XPS) of Si–graphene anode before and after 50th cycling from the discharged pouch full-cells with 0% and 5% FEC for Si 2p orbital.

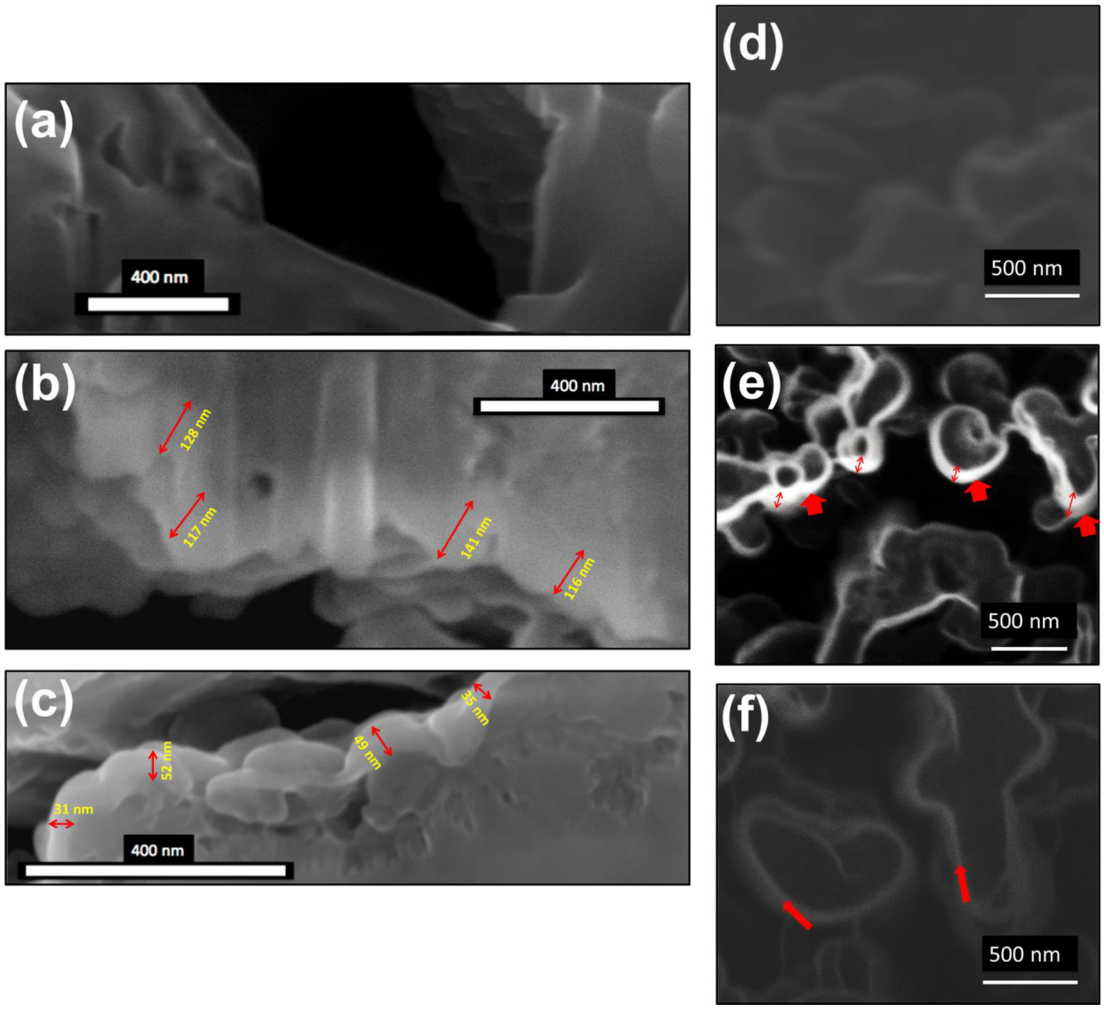

Fig. 7. FIB-SEM cross-sectional images of Si–graphene anode (a) before and after 50th cycling from the discharged pouch full-cells with (b) 0% and (c) 5% FEC in the EC–DEC (1:1 wt.%) electrolyte. Ion Beam surface images of Si–graphene anode (d) before and after 50th cycling from the discharged pouch full-cells with (e) 0% and (f) 5% FEC.

brittle, and then the crack was produced during cycling in the full-cell without FEC.

Nevertheless, both surfaces showed an increase in sizes of agglomerated particles presumably due to formation of outer SEI-like layer after cycling. The XPS analysis of Si 2p (Fig. 6) is straightforward. The pristine anode displayed two broad peaks attributed to Si–Si bonds and Si–O bonds, whereas the two cycled samples do not present any peak, indicating that an outer layer thick enough to preclude detection of interior Si was formed.

To discern this SEI-like layer more clearly, the cross-sectional images of the materials were observed by FIB-SEM. Fig. 7(a)–(c) shows the cross-sections of agglomerated Si–graphene composite particles from pristine state and from the full-cell after 50 cycles with 0% FEC and 5% FEC. The pristine electrode had no outer layer on the surface (Fig. 7(a)), whereas the cycled electrode without FEC showed the distinctly bright and rough layer on the surface (Fig. 7(b)). The layer is considered to be the SEI according the previous reported images [31,32]. The oxide layer, such as SEI with relatively low electrical conductivity, looks bright in SEM because the electron was focused on the area. As shown in Fig. 7(b) and (c), the electrode with 5% FEC had a much thinner and more uniform SEI layer compared to the cell without FEC. The thickness of SEI without FEC was 100–150 nm, whereas that with 5% FEC was 30–50 nm. This fact can also confirmed by ion-beam images of Si–graphene anode after cutting by ion-beam (Fig. 7(d)–(f)). In Fig. 7(e) and (f), it was observed that the dramatically bright outside layer was covered on the agglomerated Si–graphene particles cycled in the full-cells without FEC, whereas that with 5% FEC showed a less bright layer.

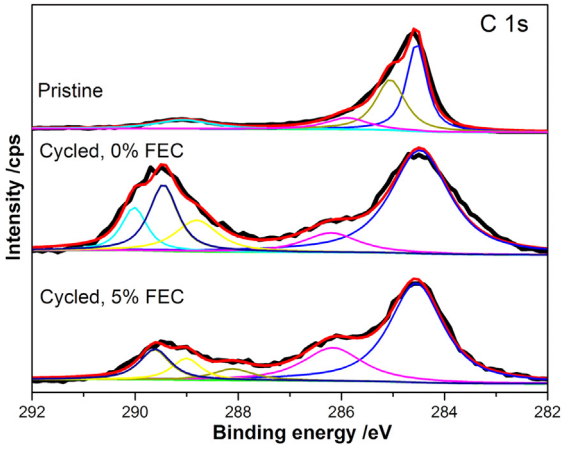

Fig. 8. X-ray photo-electron spectroscopy (XPS) of Si–graphene anode before and after 50th cycling from the discharged pouch full-cells with 0% and 5% FEC for C 1s orbital.

3.4. Effect of FEC additive on the surface composition (SEI) of Si–graphene anode (XPS)

The composition of the SEI layer on the surface of Si–graphene anode can be confirmed by XPS. Fig. 8 shows the XPS peaks obtained between 292 and 282 eV binding energy (carbon 1s orbital) of pristine and cycled Si–graphene anode from the full-cells with 0% and 5% FEC. The pristine Si–graphene showed the typical XPS C1s peaks of graphene [33]. The 284.5 eV peak is from the hexatomic C–C ring bonding of graphene. The other peaks presenting at 285.1, 286–287, and 289.0 eV correspond to C–O, C=O, and O–C=O bonding, respectively. With relatively decreasing in the intensity of the carbon oxides peaks based on that of C–C peak at 284.5 eV, the quality of graphene increased [33].

The composite Si–graphene after 50 cycles has several peaks in the oxidized binding energy of around 286–290 eV. In particular, three oxidized peaks were detected at 288–290 eV, and it was confirmed to be the SEI compounds such as CH_2OCO_2Li and Li_2CO_3 (–R–$\underline{C}H_2OCO_2Li$: 288–289 eV, –$Li_2\underline{C}O_3$: 290 eV, –R–$CH_2O\underline{C}O_2Li$: 290–291 eV [27,34,35]), which are produced by reduction of EC and DEC electrolyte [23]. With the addition of 5% FEC, the intensity (area) of the peaks corresponding to SEI compounds of CH_2OCO_2Li and Li_2CO_3 decreased greatly based on the main graphene C–C bonding peak (284.5 eV), whereas the peak of near 286 eV increased a little. Because the binding energy of near 286 eV is mostly from the single and double bonding of C and O and the intensity of peak increased by an addition of FEC, the increment is likely due to formation of polycarbonate (PC) with many C and O bonds. The polycarbonate is well known as a good SEI compound with high structural stability and high passive property from further decomposition of electrolyte and consumption of Li ions [23].

4. Conclusions

We investigated the effect of electrolyte additive of fluoroethylene carbonate (FEC) on the capacity fade of full-cells employing the Si–graphene anode and NCA cathode and optimize the FEC content in order to improve the capacity and cyclability. When FEC was added to the EC–DEC (1:1 wt.%) electrolyte in the range of 5–20 wt.% FEC, the initial cyclability and capacity of the full-cell was improved. In particular, the optimized content of FEC was 5%, which showed the highest capacity and most stable cyclability. It was attributed to the thin (30–50 μm) and uniform SEI formation with low ionic resistance (~2 ohm cm^2) on the electrode, which can depend the further dissolution of electrolyte and the exhaustion of Li-ions in the full-cell. From the cross-sectional images of Si–graphene anodes using FIB-SEM, it was confirmed that the cycled anode with 5% FEC had more than 3 times thinner SEI layer than that without FEC. From the XPS analysis, it was found that by an addition of 5% FEC the SEI compounds to consume Li ions such as CH_2OCO_2Li, Li_2CO_3, and LiF decreased, and polycarbonate (PC) with high stability and good passive property increased. However, 2.5% FEC did not exhibit the positive effects (similar behavior with the cell without FEC) likely due to less production of PC and more than 10% FEC showed less improvement than 5% FEC due to more production of LiF to consume Li ions in the full-cells.

Acknowledgments

This research was supported by 'DOE SBIR Program (USA)' and 'National Research Foundation of Korea' (2012R1A6A3A03040261).

References

[1] M. Armand, J.M. Tarascon, Nature 451 (2008) 652–657.
[2] V. Etacheri, R. Marom, R. Elazari, G. Salitra, D. Aurbach, Energy Environ. Sci. 4 (2011) 3243–3262.
[3] C.K. Chan, H. Peng, G. Liu, K. McIlwrath, X.F. Zhang, R.A. Huggins, Y. Cui, Nat. Nano 3 (2008) 31–35.
[4] M. Ge, J. Rong, X. Fang, C. Zhou, Nano Lett. 12 (2012) 2318–2323.
[5] A. Magasinski, P. Dixon, B. Hertzberg, A. Kvit, J. Ayala, G. Yushin, Nat. Mater. 9 (2010) 353–358.
[6] H. Zhang, P.V. Braun, Nano Lett. 12 (2012) 2778–2783.
[7] J.K. Lee, K.B. Smith, C.M. Hayner, H.H. Kung, Chem. Commun. 46 (2010) 2025–2027.
[8] Y.S. He, P.F. Gao, J. Chen, X.W. Yang, X.Z. Liao, J. Yang, Z.F. Ma, RSC Adv. 1 (2011) 958–960.
[9] X. Zhao, C.M. Hayner, M.C. Kung, H.H. Kung, Adv. Energy Mater. 1 (2011) 1079–1084.
[10] X. Xin, X. Zhou, F. Wang, X. Yao, X. Xu, Y. Zhu, Z. Liu, J. Mater. Chem. 22 (2012) 7724–7730.
[11] X. Zhou, A.-M. Cao, L.-J. Wan, Y.-G. Guo, Nano Res. 5 (2012) 845–853.
[12] Y. Zhu, W. Liu, X. Zhang, J. He, J. Chen, Y. Wang, T. Cao, Langmuir 29 (2012) 744–749.
[13] S.-L. Chou, J.-Z. Wang, M. Choucair, H.-K. Liu, J.A. Stride, S.-X. Dou, Electrochem. Commun. 12 (2010) 303–306.
[14] H.-C. Tao, L.-Z. Fan, Y. Mei, X. Qu, Electrochem. Commun. 13 (2011) 1332–1335.
[15] L. Ji, H. Zheng, A. Ismach, Z. Tan, S. Xun, E. Lin, V. Battaglia, V. Srinivasan, Y. Zhang, Nano Energy 1 (2012) 164–171.
[16] J.-G. Ren, Q.-H. Wu, G. Hong, W.-J. Zhang, H. Wu, K. Amine, J. Yang, S.-T. Lee , Energy Technol. 1 (2013) 77–84.
[17] L.J. Fu, H. Liu, C. Li, Y.P. Wu, E. Rahm, R. Holze, H.Q. Wu, Solid State Sci. 8 (2006) 113–128.
[18] A. Barré, B. Deguilhem, S. Grolleau, M. Gérard, F. Suard, D. Riu, J. Power Sources 241 (2013) 680–689.
[19] N. Dimov, K. Fukuda, T. Umeno, S. Kugino, M. Yoshio, J. Power Sources 114 (2003) 88–95.
[20] W.R. Liu, J.H. Wang, H.C. Wu, D.T. Shieh, M.H. Yang, N.L. Wu, J. Electrochem. Soc. 152 (2005) A1719–A1725.
[21] Y.M. Kang, J.Y. Go, S.M. Lee, W.U. Choi, Electrochem. Commun. 9 (2007) 1276–1281.
[22] R. Ruffo, S.S. Hong, C.K. Chan, R.A. Huggins, Y. Cui, J. Phys. Chem. C 113 (2009) 11390–11398.
[23] V. Etacheri, O. Haik, Y. Goffer, G.A. Roberts, I.C. Stefan, R. Fasching, D. Aurbach, Langmuir 28 (2011) 965–976.
[24] N.-S. Choi, Y. Lee, S.-S. Kim, S.-C. Shin, Y.-M. Kang, J. Power Sources 195 (2010) 2368–2371.
[25] Y.-M. Lin, K.C. Klavetter, P.R. Abel, N.C. Davy, J.L. Snider, A. Heller, C.B. Mullins, Chem. Commun. 48 (2012) 7268–7270.
[26] K. Eom, T. Joshi, A. Bordes, I. Do, T.F. Fuller, J. Power Sources 249 (2014) 118–124.
[27] H. Nakai, T. Kubota, A. Kita, A. Kawashima, J. Electrochem. Soc. 158 (2011) A798–A801.
[28] S.S. Zhang, K. Xu, T.R. Jow, Electrochim. Acta 49 (2004) 1057–1061.
[29] L. Chen, K. Wang, X. Xie, J. Xie, J. Power Sources 174 (2007) 538–543.
[30] E.-G. Shim, T.-H. Nam, J.-G. Kim, H.-S. Kim, S.-I. Moon, J. Power Sources 175 (2008) 533–539.
[31] Z. Du, S. Zhang, T. Jiang, R. Lin, J. Zhao, Electrochim. Acta 74 (2012) 222–226.
[32] J.T. Lee, N. Nitta, J. Benson, A. Magasinski, T.F. Fuller, G. Yushin, Carbon 52 (2013) 388–397.
[33] H. Huang, Y. Xia, X. Tao, J. Du, J. Fang, Y. Gan, W. Zhang, J. Mater. Chem. 22 (2012) 10452–10456.
[34] A.M. Andersson, A. Henningson, H. Siegbahn, U. Jansson, K. Edström, J. Power Sources 119–121 (2003) 522–527.
[35] M. Lu, H. Cheng, Y. Yang, Electrochim. Acta 53 (2008) 3539–3546.